



Towards left-handed metamaterials using single-size dielectric resonators: The case of TiO₂-disks at millimeter wavelengths

R. Yahiaoui, U.-C. Chung, C. Elissalde, M. Maglione, V. Vigneras, and P. Mounaix

Citation: [Applied Physics Letters](#) **101**, 042909 (2012); doi: 10.1063/1.4739498

View online: <http://dx.doi.org/10.1063/1.4739498>

View Table of Contents: <http://scitation.aip.org/content/aip/journal/apl/101/4?ver=pdfcov>

Published by the [AIP Publishing](#)



Re-register for Table of Content Alerts

Create a profile.



Sign up today!



Towards left-handed metamaterials using single-size dielectric resonators: The case of TiO₂-disks at millimeter wavelengths

R. Yahiaoui,^{1,2,a)} U.-C. Chung,^{3,4} C. Elissalde,³ M. Maglione,³ V. Vigneras,² and P. Mounaix¹

¹LOMA, University of Bordeaux, CNRS, UMR 5798, 351 cours de la Libération, F-33405 Talence Cedex, France

²IMS, University of Bordeaux, CNRS, UMR 5218, 16 Avenue Pey Berland, 33600 Pessac Cedex, France

³ICMCB, University of Bordeaux, CNRS, UPR 9048, 87 Avenue du Docteur Albert Schweitzer, 33600 Pessac Cedex, France

⁴CRPP, University of Bordeaux, CNRS, UPR 9048, 115 Avenue du Docteur Albert Schweitzer, 33600 Pessac Cedex, France

(Received 8 May 2012; accepted 13 July 2012; published online 27 July 2012)

We report a strong magnetic activity using an all-dielectric metamaterial based on Mie resonances, designed to work at millimeter wavelengths over the 30–70 GHz band. A good agreement was achieved between numerical simulations and experiment in the case of one meta-layer based on TiO₂-disks, manufactured using a simple bottom-up approach. We also demonstrate through numerical simulations a negative refractive index within the same investigated metamaterial made of high dielectric permittivity single-size pellets. Choosing the suitable aspect-ratio of the metamaterial building blocks, a broadband magnetic response and a left-handed behavior are simultaneously obtained. This is a promising step towards innovative and complex electromagnetic functions, involving cheap and easy made metamaterials for millimeter wave applications. © 2012 American Institute of Physics. [<http://dx.doi.org/10.1063/1.4739498>]

Over the last decade, metamaterials with their unusual properties have allowed an amazing breakthrough in the field of physics. They have been explored in many potential applications such as sub-diffraction-limited imaging,¹ biosensing,² medical imaging,³ and so on. Conventional method used to fabricate metamaterials by integrating sub-wavelength metallic patterns in a dielectric matrix (relying on cleanroom and microelectronics facilities) is difficult to achieve, particularly for unit cells of complex geometry with sub-micron or nano-scale sizes. Other drawbacks of the basic top-down approach are the dramatic losses induced by heat treatments, uncontrolled chemical reaction during processing, and anisotropy of the metallic inclusions. Recently, all-dielectric (AD) metamaterials based on the Mie resonances of high-dielectric permittivity materials have been the subject of intense research activity.^{4–7} Indeed, this category of metamaterials offers an alternative and an interesting way to achieve simultaneously low-loss and homogeneous metamaterials. Additionally, the bandwidth of a metamaterial response is an important criterion that may be very valuable in various applications such as band pass filters, wavelength division multiplexers, and antenna-systems. Most of the other types of metamaterials operate intrinsically within a very narrow frequency ranges. To target this goal, multiple-band metamaterials have been demonstrated with specific narrow frequencies,^{8–10} however, broad bandwidth metamaterials still remain a challenge. In this letter, we have designed and experimentally demonstrated at microwave frequencies a broadband magnetic activity within an all-dielectric metamaterial. We also demonstrate through numerical calculations that our investigated metamaterial composed of one kind of dielectric objects with single size, behaves as a left-handed medium. Titanium dioxide

(TiO₂) was used to manufacture dielectric resonators, for its high permittivity and moderate loss-level at microwave frequencies ($\epsilon \sim 92$, $\tan \delta \sim 0.05$).

Commercial TiO₂ powders were pressed into pellets, and then sintered in a furnace at 1300 °C for 4 h under oxygen-enriched atmosphere to reach well densified ($\sim 98\%$) disks of about 3.3 mm in diameter. These latter were finally polished to reduce the thickness to about 460 μm , and to obtain perfect parallel faces. 160 dielectric resonators have been elaborated (Fig. 1(a)). The resulting dielectric resonators were then set in an array of holes, as shown in Fig. 1(b). The holes were made mechanically through a 1 mm thick Rohacell[®] substrate ($\epsilon \sim 1.02$, $\tan \delta \sim 1\%$)¹¹ using a drilling machine with an optimal periodicity of $P = 4.5$ mm along E_{inc} and H_{inc} directions.

Numerical simulations based on finite element method (HFSS) have been performed in order to predict the electromagnetic response of our metamaterial. We consider here the case of a single meta-layer along the direction of propagation k , illuminated at normal incidence. The appropriate polarizations of the electric and magnetic fields are shown in Fig. 1(b). The numerical effective parameters retrieved by the inversion of Fresnel equations,¹² for different values of the diameter d of the disks, are given in Fig. 2. Note that the periodicity P of the lattice is modified in each case to keep constant the filling factor (i.e., $FF = 42\%$). The permeability is highly dispersive and exhibits a Lorentz-like resonant behavior. For diameter $d \geq 2$ mm, the position of the first Mie resonance does not shift significantly and it is mainly imposed by the thickness t of the disks.

By contrast, upon increasing d , the distance between the first and higher order modes decreases, and by making sure that $d \gg t$, the resonances can overlap, which gives rise to a much-broader continuous band of negative μ (Fig. 2(a)).

^{a)}Electronic mail: p.mounaix@loma.u-bordeaux1.fr.

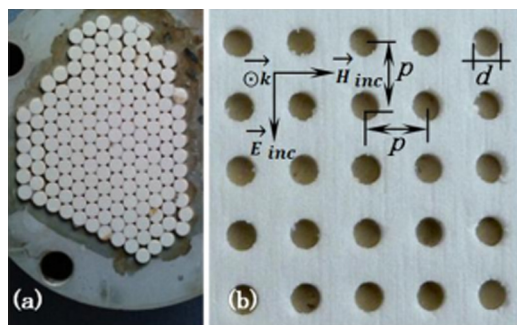


FIG. 1. Photograph of the fabricated TiO_2 disks (a). Photograph of the simple square lattice dielectric resonators, embedded in a 1 mm thick Rohacell[®] matrix (b), the relevant geometrical dimensions are: diameter $d = 3.3$ mm, period $p = 4.5$ mm, thickness $t = 460$ μm .

Furthermore, the dielectric losses ($\tan \delta$) contribute favourably to the broadening of the spectral region of negative μ . We have already demonstrated this apparently counter-intuitive effect using a SrTiO_3 rods-based metamaterial at terahertz frequencies.¹³ The electric permittivity goes gradually from a static and weakly dispersive to a strongly resonant behaviour (see Fig. 2(b)).

Microwave measurements using a vector network analyzer and horn antennas in a quasi-optical configuration have been carried out in the 30–70 GHz band on an experimental demonstrator, with the following geometrical dimensions: $d = 3.3$ mm, $t = 460$ μm , and $FF = 42\%$ corresponding to $P = 4.5$ mm, thus offering the best compromise in terms of continuous-bandwidth and depth of negative μ , as expected in Fig. 3(a). The resulting experimental effective parameters (dashed lines) are in excellent agreement with the simulated ones (solid lines) (see Figs. 3(c) and 3(d)). μ' exhibits negative values from 35.7 GHz to 36.63 GHz and from 37.4 GHz to 40.6 GHz, approximately in both simulation and experiment (Fig. 3(c)). One can observe a minor shift towards low frequencies in the measured spectrum of the effective ϵ

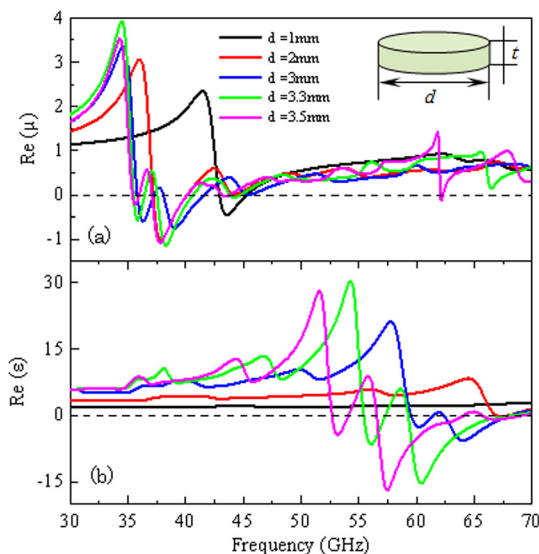


FIG. 2. Evolution of the simulated effective parameters for different values of the diameter of the disks: $d = 1, 2, 3, 3.3,$ and 3.5 mm, respectively. The filling factor FF was set to about 42% in each case. (a) Permeability, the unit cell of the metamaterial is indicated in the inset, (b) permittivity.

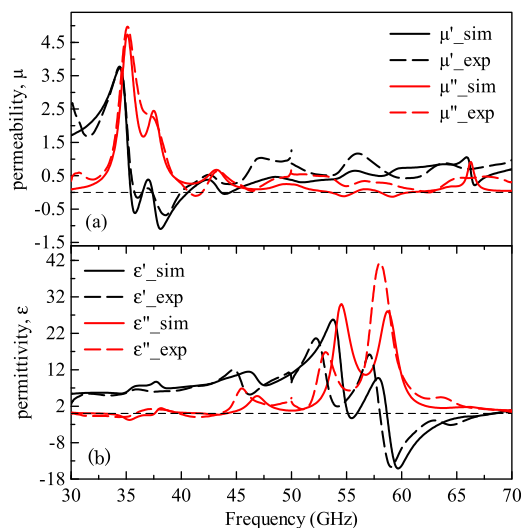


FIG. 3. Simulated (solid lines) and measured (dashed lines) magnetic permeability (a), electric permittivity (b) for $d = 3.3$ mm, $t = 460$ μm , and $FF = 42\%$ corresponding to $p = 4.5$ mm.

compared to the simulated one, which exhibits negative values over a wide frequency band from 59 GHz to 68.9 GHz, approximately (Fig. 3(d)). The settled geometrical diameter in both simulation and experiment ($d = 3.3$ mm) does not provide the metamaterial with negative refractive index, since negative μ' and negative ϵ' do not overlap in frequency.

The most common method used to obtain effective double negative media (DNG) with AD metamaterials is to combine sets of resonators with two different sizes.^{14,15} The negative refractive index is then expected in the frequency region where resonance of TM mode in one of both sets of particles and TE mode in the other are simultaneously present.¹⁶ In our case, we highlight the originality of using an array of identical dielectric resonators in the processing of a double negative metamaterial. The thickness of the disks was optimized and settled to 420 μm for an operating frequency of about 40 GHz and we further performed numerical calculations to assess the role and the impact of the periodicity P on the effective parameters, taking into account the actual geometrical dimensions of the unit cell of the metamaterial (i.e., $t = 420$ μm , $d = 3.3$ mm). The result of our numerical investigations showed that a negative refractive index can be achieved by increasing the periodicity P (i.e., reducing the filling factor, see Fig. 4(c)). The negative refractive index is possible, because the target frequency of the negative ϵ (Fig. 4(b)) coincides with a negative μ , induced by additional higher resonances in the permeability spectrum around 50 GHz, 60 GHz, and 66 GHz, respectively, for $P \leq 6$ mm (see Fig. 4(a)). The spectral bandwidth of the negative refractive index moves towards low frequencies, thus, proportionally to the periodicity P . The frequency range of the negative μ initially extended over a broadband is modified and becomes positive. The refractive index is expressed in terms of the permittivity and permeability as $n = \pm \sqrt{\epsilon_1 \mu_1 - \epsilon_2 \mu_2 + i(\epsilon_1 \mu_2 + \epsilon_2 \mu_1)}$. It is possible to achieve a negative refractive index if $\epsilon_1 \mu_2$ is larger than $\epsilon_2 \mu_1$, which is effectively the case near resonances, the metamaterial is then considered as a single negative material (i.e., $\mu_1 > 0$ and $\epsilon_1 < 0$).¹⁷ The figure of merit (FOM) of a

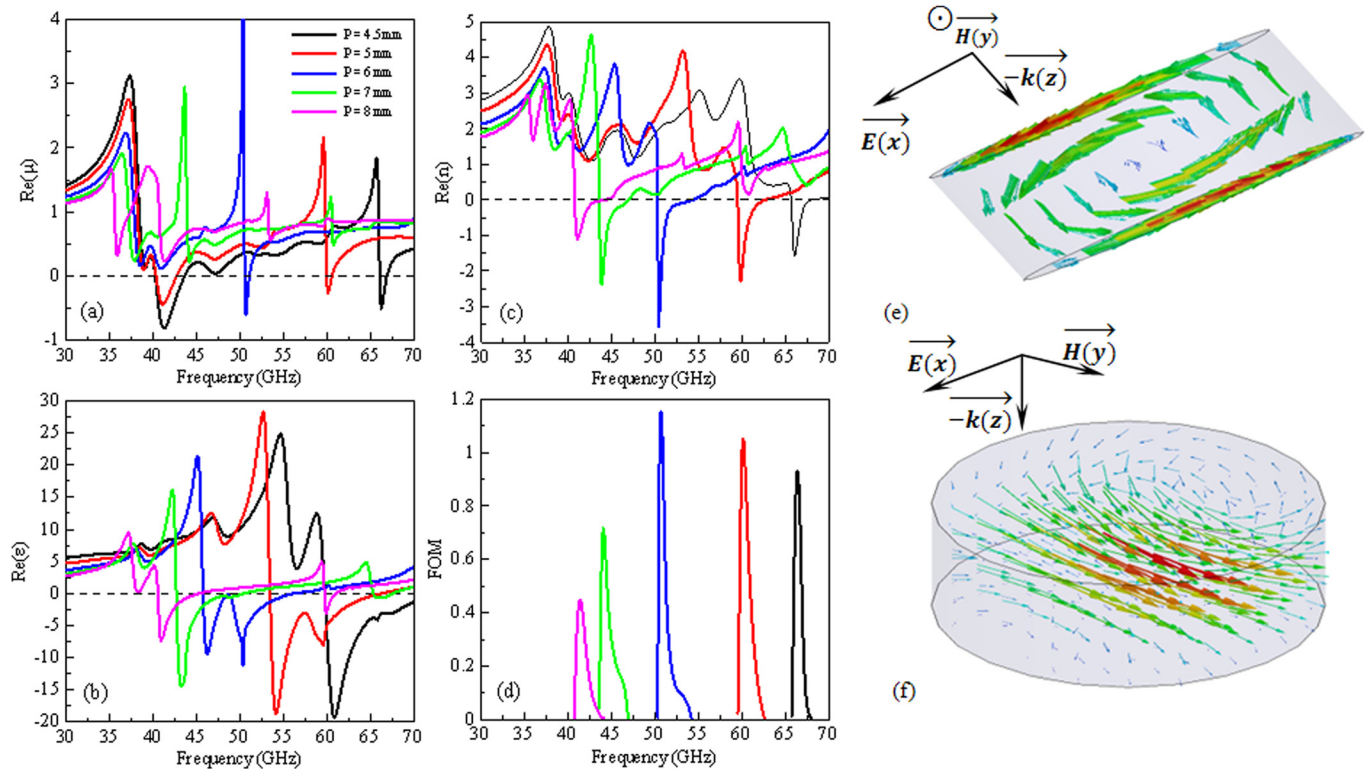


FIG. 4. Simulated real parts of effective parameters (a) permeability, (b) permittivity, (c) refractive index, (d) distribution of the FOM in the negative refractive index band for the case: $t = 420 \mu\text{m}$, $d = 3.3 \text{ mm}$ and for different values of the period $P = 4.5 \text{ mm}$, 5 mm , 6 mm , 7 mm , and 8 mm , (e)-(f) distribution of the electric field E and the magnetic field H , respectively, within the unit cell of the metamaterial at 37.7 GHz , the polarization of the incident electromagnetic wave is also given.

metamaterial is usually defined as $|\text{Re}(n)|/|\text{Im}(n)|$. It is mainly considered as a losses-indicator, which evaluates the “quality” of the negative refraction. In our case, the FOM is expected to be lower compared to the case, where μ and ϵ present high negative values simultaneously. Fig. 4(d) shows the distribution of the FOM around the negative refractive index region. Basically, large values are associated with small losses and from our simulation results, the maximum value reached is $\text{FOM} = 1.15$ around 50.7 GHz , corresponding to $\text{Re}(n) \sim -2.2$, when $P = 6 \text{ mm}$ (see Fig. 4(d)). Other works have reported structures with $\text{FOM} > 1$.^{18,19}

The resonant behavior is closely connected to the large value of the material permittivity. To give physical understanding of this phenomenon, the electric and magnetic field patterns inside one unit cell of the disks array for the first Mie resonance 37.7 GHz (Fig. 4(a)) are plotted in Figs. 4(e) and 4(f). The wave front of an incident plane wave undergoes a strong distortion close to the metamaterial in order to satisfy simultaneously the continuity and discontinuity conditions of tangential and normal electric-field components at the disk-air interfaces, respectively. The electric field, which develops inside a disk, is predominantly tangential close to the surface of the disk. This leads to the creation of dispersive Eddy currents within the disk, as shown in Fig. 4(e), which enhance the magnetic field in the disk polarized along the y axis, as shown in Fig. 4(f). A resonant behavior is then expected at the specific frequency, thus, giving rise to a negative magnetic permeability μ' .⁵

In summary, inexpensive bottom-up approach was used to fabricate dielectric resonators out of TiO_2 nanoparticles.

Our investigated metamaterial was arranged in a square lattice of disks with unique sizes. By the appropriate choice of a large aspect-ratio of the disks ($d \gg t$), we proposed an original approach for achieving simultaneously a broadband magnetic activity, with a left-handed behavior. The next step would be to tune this design for higher frequencies.

This work has been performed at the University of Bordeaux 1 within the framework of the Project: GIS-AMA-SAMM. The authors would like to thank M. Eddie Maillard for manufacturing the Rohacell[®] matrix, with the mechanical LOMA facilities.

¹N. Fang, H. Lee, C. Sun, and X. Zhang, *Science*, **308**, 534 (2005).

²K. Kneipp, H. Kneipp, I. Itzkan, R. R. Dasari, and M. S. Feld, *J. Phys.: Condens. Matter*, **14**, 597 (2002).

³M. J. Freire, R. Marques, and L. Jelinek, *Appl. Phys. Lett.*, **93**, 231108 (2008).

⁴Q. Zhao, L. Kang, B. Du, H. Zhao, Q. Xie, X. Huang, B. Li, J. Zhou, and L. Li, *Phys. Rev. Lett.*, **101**, 027402 (2008).

⁵H. Němec, P. Kužel, F. Kadlec, C. Kadlec, R. Yahiaoui, and P. Mounaix, *Phys. Rev. B*, **79**, 241108 (2009).

⁶Q. Zhao, J. Zhou, F. Zhang, and D. Lippens, *Mater. Today*, **12**, 60 (2009).

⁷H. Němec, C. Kadlec, F. Kadlec, P. Kužel, R. Yahiaoui, U.-C. Chung, C. Elissalde, M. Maglione, and P. Mounaix, *Appl. Phys. Lett.*, **100**, 061117 (2012).

⁸Y. Yuan, C. Bingham, T. Tyler, S. Palit, T. H. Hand, W. J. Padilla, N. M. Jokerst, and S. A. Cummer, *Appl. Phys. Lett.*, **93**(19), 191110 (2008).

⁹C. Sabah, *Microwave Opt. Technol. Lett.*, **53**, 2255 (2011).

¹⁰H. Li, L. H. Yuan, B. Zhou, X. P. Shen, Q. Cheng, and T. J. Cui, *J. Appl. Phys.*, **110**, 014909 (2011).

¹¹C. Roman, O. Ichim, L. Sarger, V. Vigneras, and P. Mounaix, *Electron. Lett.*, **40**, 1167 (2004).

- ¹²D. R. Smith, S. Schultz, P. Markoš, and C. M. Soukoulis, *Phys. Rev. B* **65**, 195104 (2002).
- ¹³R. Yahiaoui, H. Němec, P. Kužel, F. Kadlec, C. Kadlec, and P. Mounaix, *Opt. Lett.* **34**, 3541 (2009).
- ¹⁴K. Shibuya, K. Takano, N. Matsumoto, K. Izumi, H. Miyazaki, Y. Jimba, and M. Hangyo, in *Proceedings of Metamaterials, Pamplona, 2008* (Metamorphose, 2008), p. 777.
- ¹⁵T. Lepetit, E. Akmonsoy, and J.-P. Ganne, *Appl. Phys. Lett.* **95**, 121101 (2009).
- ¹⁶O. G. Vendik, M. S. Gashinova, in *Proceeding of 34th European Microwave Conference, Amsterdam, 2004* (Horizon House Publications, 2004), pp. 1209–1212.
- ¹⁷R. A. Depine and A. Lakhtakia, *Microwave Opt. Technol. Lett.* **41**, 315 (2004).
- ¹⁸S. Zhang, W. Fan, N. C. Panoiu, K. J. Malloy, R. M. Osgood, and S. R. J. Brueckel, *Phys. Rev. Lett.* **95**, 137404 (2005).
- ¹⁹S. Zhang, W. Fan, K. J. Malloy, S. R. J. Brueckel, N. C. Panoiu, and R. M. Osgood, *J. Opt. Soc. Am. B* **23**, 434 (2006).